Available online at www.sciencedirect.com
ScienceDirect
Journal of the European Ceramic Society 29 (2009) 1535–1542
www.elsevier.com/locate/jeurceramsoc

Correlation of wear behavior and indentation fracture resistance in silicon nitride ceramics hot-pressed with alumina and yttria

Hiroyuki Miyazaki *, Hideki Hyuga, Yu-ichi Yoshizawa, Kiyoshi Hirao, Tatsuki Ohji

National Institute of Advanced Industrial Science and Technology (AIST), Anagahora 2266-98, Shimo-shidami, Moriyama-ku, Nagoya 463-8560 Japan

Received 2 July 2008; received in revised form 14 August 2008; accepted 15 August 2008
Available online 24 September 2008

Abstract

Nine kinds of silicon nitrides with different microstructures were fabricated by controlling both sintering conditions and amounts of sintering additives, Al_2O_3 and Y_2O_3. The wear behavior of the various Si_3N_4 ceramics was investigated in sliding contact test without lubricant. The specific wear rate varied notably from 6×10^{-6} to 4×10^{-4} $mm^3\ N^{-1}\ m^{-1}$ depending on the microstructures, whose ranking was difficult to predict directly from the hardness or fracture resistance obtained by the indentation fracture (IF) technique as well as the single-edge-precracked beam (SEPB) method. A good correlation was obtained between the specific wear rate and both mechanical properties when a lateral-crack chipping model was applied as the material removal process. However, the correlation was lost when the fracture toughness obtained by the SEPB method was employed, indicating that the conventional long-crack toughness is inappropriate for analyzing the wear behavior of Si_3N_4 exhibiting a rising *R*-curve behavior.

Keywords: Si_3N_4; Wear resistance; Toughness and toughening; Hardness; Indentation fracture technique

1. Introduction

Silicon nitride is an attractive material for tribological applications since it possesses superior wear resistance and advantages such as light weight, high strength and toughness, good corrosion resistance and a low thermal expansion coefficient. Many studies have been conducted to improve its mechanical properties through microstructural control, such as "self-reinforcing" mechanism. Although there has been much research on the tribological behavior of silicon nitride, many of them have been focused on the relation between the sliding environment and the wear resistance,[1–9] and relatively fewer studies have explored the effect of microstructure on the wear performance.[4,10–13] However, the reported relationships between microstructure and tribological performance are often contradictory, leaving fundamental understanding of its wear mechanism to be clarified. For example, Zutshi et al., Gomes et al. and Doğan and Hawk found that the wear resistance was improved when the grain size became smaller despite of a decrease in fracture toughness.[10–12] By contrast, Carrasquero et al. demonstrated that the "self-reinforced" microstructure with elongated grains suppressed the propagation of cracks, which not only improved both fracture toughness and strength but also enhanced the wear resistance.[13] In the case of silicon carbide whisker-reinforced silicon nitride composites, Wang and Mao reported that the pullout mechanism of SiC whisker made the composite more wear resistant than the monolithic silicon nitride,[14] while Gomes et al. and Doğan and Hawk observed little difference between the wear performances for them.[15,16] In our previous studies, the influence of microstructure on the friction and wear properties of various Si_3N_4 ceramics was investigated in sliding contact test without lubricant.[17,18] It was found that the tribological properties varied considerably depending on the microstructures. However, a clear relationship between the tribological characteristics and the grain size as well as the mechanical properties was not obtained.

The complicated results from all these researches may be attributable to the complexity of the experimental conditions, especially to the diversity of the samples tested in these literatures, that is, the chemical composition and crystallinity of the intergranular phase as well as the ratio of α/β phase of silicon

* Corresponding author. Tel.: +81 52 7367486; fax: +81 52 7367405.
E-mail address: h-miyazaki@aist.go.jp (H. Miyazaki).

0955-2219/$ – see front matter © 2008 Elsevier Ltd. All rights reserved.
doi:10.1016/j.jeurceramsoc.2008.08.020

nitride were different besides variations in the grain size distribution and morphology.[11,12] In this study, in order to elucidate the effect of the grain size and morphology on the tribological property, nine silicon nitride samples were hot-pressed using equal amounts of alumina and yttria as sintering additives to yield an intergranular amorphous phase with almost the same chemical composition, while the distribution of grain size was controlled by both sintering conditions and total amounts of additives. The samples were tested in unlubricated sliding test at an ambient atmosphere to correlate the volume wear loss to both microstructures and mechanical properties such as hardness and fracture toughness. An indentation fracture model for material removal process in abrasive wear, which was developed by Evans and Marshall,[19] was employed to explain the dependence of the wear volume on an inverse function of the hardness and fracture toughness.

2. Experimental procedure

2.1. Materials

Two sets of silicon nitride ceramics (listed in Table 1) were fabricated from Si_3N_4 powder with Y_2O_3 and Al_2O_3 as sintering additives. The amounts of the sintering additives of the first set of samples (A series) were fixed at 5 wt% Al_2O_3/5 wt% Y_2O_3. In order to alter both grain size distributions and grain morphologies of the silicon nitride samples, the combination of the sintering temperature and soaking time was varied as follows; 1750 °C for 1 h, 1850 °C for 1 h, 1950 °C for 2 h and 1950 °C for 8 h. By contrast, the amount of additives of the second set of samples was increased progressively from 1 wt% Al_2O_3/1 wt% Y_2O_3 to 10 wt% Al_2O_3/10 wt% Y_2O_3 while the sintering condition was set constant at 1950 °C for 2 h (B series). The ratios of Y_2O_3 to Al_2O_3 in weight percent were kept at unity for all compositions, so that the chemical compositions of intergranular phases were considered to be almost identical. However, the content of silica from the silica on the surface of raw Si_3N_4 powder was supposed to decrease slightly with an increase in the additives. The percentage of nitrogen in the glass phase might also vary depending on the compositions. The starting powders were mixed in ethanol for 24 h. The slurry was dried and passed through a 150-mesh sieve. The mixed powders were hot-pressed in a graphite furnace at temperatures ranging from 1750 to 1950 °C under a pressure of 30 MPa in a nitrogen atmosphere. The detailed fabrication procedure was described in our previous reports.[17,18] The densities of the as-sintered bodies were measured using the Archimedes technique. The crystal phases in the specimens were identified by X-ray diffraction (XRD). The machined samples were polished and plasma etched in CF_4 gas before microstructural observation by scanning electron microscopy (SEM). The diameter of each grain was evaluated by the shortest grain diagonal in two-dimensional images with magnifications of 10k and/or 5k. In order to count coarse and elongated grains (major axis $\gtrsim$8 μm) which occasionally appeared in the samples sintered at higher temperatures, the micrographs with the lower magnification of 1k were also used. Aspect ratios of the normal grains were estimated from the mean value of the 10% highest observed aspect ratios.[20] Aspect ratios of the coarse grains selected from the micrographs at a magnification of 1k were calculated by the same procedure as mentioned above.

2.2. Test procedure

Young's modulus was measured by the ultrasonic pulse echo method as used in Japanese industrial standard (JIS) R 1602.[21] Vickers indentations were made on the polished surface perpendicular to the hot-pressing axis with a hardness tester (Model AVK-C2, Akashi Corp., Yokohama, Japan). Both Vickers hardness and indentation fracture resistance were evaluated at a load of 294 N with the dwell time of 15 s. Eight impressions were made for each sample. The lengths of the impression diagonals, $2a$, and sizes of surface cracks, $2c$, were measured with a traveling microscope (Model MM-40, Nikon Corp., Tokyo, Japan) immediately after the unloading. A 10× eyepiece and a 50× objective were used to observe the bright field images of the indentations. The fracture resistance, K_R, was calculated using the Miyoshi's equation as follows,[22,23] since it was reported that

Table 1
Composition of the starting powders, sintering conditions, median grain diameter and aspect ratio of the silicon nitride samples hot-pressed with alumina and yttria as sintering additives

Material designation	Amount of sintering additives (wt%)		Sintering condition		Median grain diameter (μm)	Aspect ratio[a]	
	Al_2O_3	Y_2O_3	Temperature (°C)	Soak time (h)		Normal grain	Coarse grain
A1	5.0	5.0	1750	1	0.23	4.5	–
A2	5.0	5.0	1850	1	0.28	4.9	–
A3	5.0	5.0	1950	2	0.52	4.9	12.0
A4	5.0	5.0	1950	8	0.91	5.5	9.3
B1	1.0	1.0	1950	2	0.35	4.1	5.2
B2	1.75	1.75	1950	2	0.34	4.7	5.6
B3	2.5	2.5	1950	2	0.40	4.7	10.4
B4	3.34	3.34	1950	2	0.32	4.5	10.4
B5	10.0	10.0	1950	2	0.59	5.9	11.3

[a] The aspect ratios of the normal grains were obtained from the 5k and 10k magnification images, whereas those of coarse grains were calculated using the selected grains with major axis >8 μm in micrographs of 1k magnification.

the Miyoshi's equation gave the closest value to that obtained by the SEPB technique for silicon nitride ceramics with almost flat *R*-curve behavior.[24–27]

$$K_R = 0.018(E/H)^{1/2} Pc^{-3/2} \quad (1)$$

where E is Young's modulus and H is the Vickers hardness. P is the indentation load and c is the half-length of as-indented surface crack length. For fracture toughness, K_{Ic}, measurement, rectangular specimens (4 mm in width × 3 mm in breadth × ~40 mm in length) were machined from each sintered sample. The SEPB test was conducted in accordance with Japanese industrial standard (JIS) R 1607 with a pop-in crack depth of about 2 mm.[22]

Tribological properties were evaluated using an unlubricated ball-on-disk experiment. The samples for wear analysis were cut and grinded into plates of dimensions 30 mm × 27 mm × 5 mm and polished to surface roughness of $R_a = 0.005$ μm. A commercial Si_3N_4 ball (Nihon ceratec Co. Ltd.) with diameter of 5 mm was pushed against the sample plate with a normal load, F_n of 49 N. Wear test conditions were as follows: sliding speed = 0.18 m s^{-1}; sliding distance, L = 108 m; atmosphere = air; temperature = 22–28 °C; relative humidity during testing = 20–30%RH. Wear volumes, V, were measured using a surface profilometer and calculated according to the method of JIS R 1613.[28] Specific wear rates, W_s, were obtained by dividing V by F_nL. Two to three specimens were tested for each sample to give the average of W_s.

3. Results

3.1. Microstructure

The porosities of all the samples were less than 2%, indicating that these ceramics were almost fully densified. Fig. 1 shows SEM micrographs of the plasma-etched A-series samples sintered at different conditions using additives of 5 wt% Al_2O_3/5 wt% Y_2O_3. When the sintering temperature was 1750 and 1850 °C, the microstructures of both samples were fine and uniform (Fig. 1 A2). The grain size increased and some elongated grains appeared in the A3 sample which was sintered at 1950 °C for 2 h. Grains grew markedly and large elongated grains were formed after heating at 1950 °C for 8 h (A4 sample). In the case of B1–B5 samples which were sintered at 1950 °C for 2 h, the microstructures were almost the same except the B5 sample which consisted of large elongated grains (Fig. 2). All these microstructural characters were quantitatively evaluated by the image analysis using the SEM photographs. The resultant distributions of grain size and median diameters for those samples are shown in Fig. 3 and Table 1, respectively. The widths of grain size distribution of the A1 and A2 samples were almost the same and very narrow, 0.05–0.8 μm, while the distributions for the A4 sample shifted much higher side in *X*-axis, accompanied by the broadening of the distribution from 0.3 to 5 μm. The A3 sample showed the intermediate distribution. These features were reflected in the median diameter values listed in Table 1. By contrast, although the median diameters for B1, B2, B3 and B4 samples in Table 1 showed similar values, the differences appeared in the upper parts of the distributions; the more the amounts of additives increased, the larger the maximum grain size became (Fig. 3). The curve of grain size distribution for the B5 sample resided in the highest side in *X*-axis, which was corresponding to the coarse microstructure observed in the SEM micrographs (Fig. 2). The aspect ratios

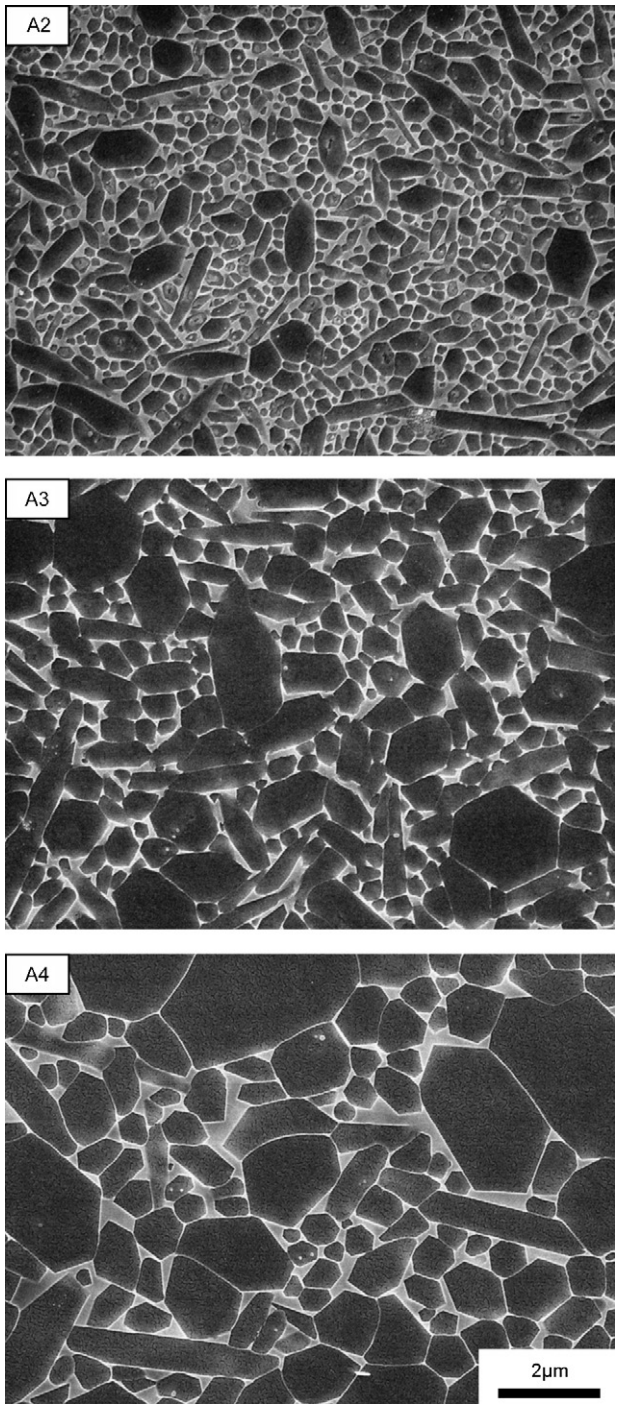

Fig. 1. SEM micrographs of Si_3N_4 hot-pressed with addition of 5 wt% Al_2O_3/5 wt% Y_2O_3 as sintering aids. The sintering condition for each sample was as follows: 1850 °C for 1 h (A2); 1950 °C for 2 h (A3); and 1950 °C for 8 h (A4).

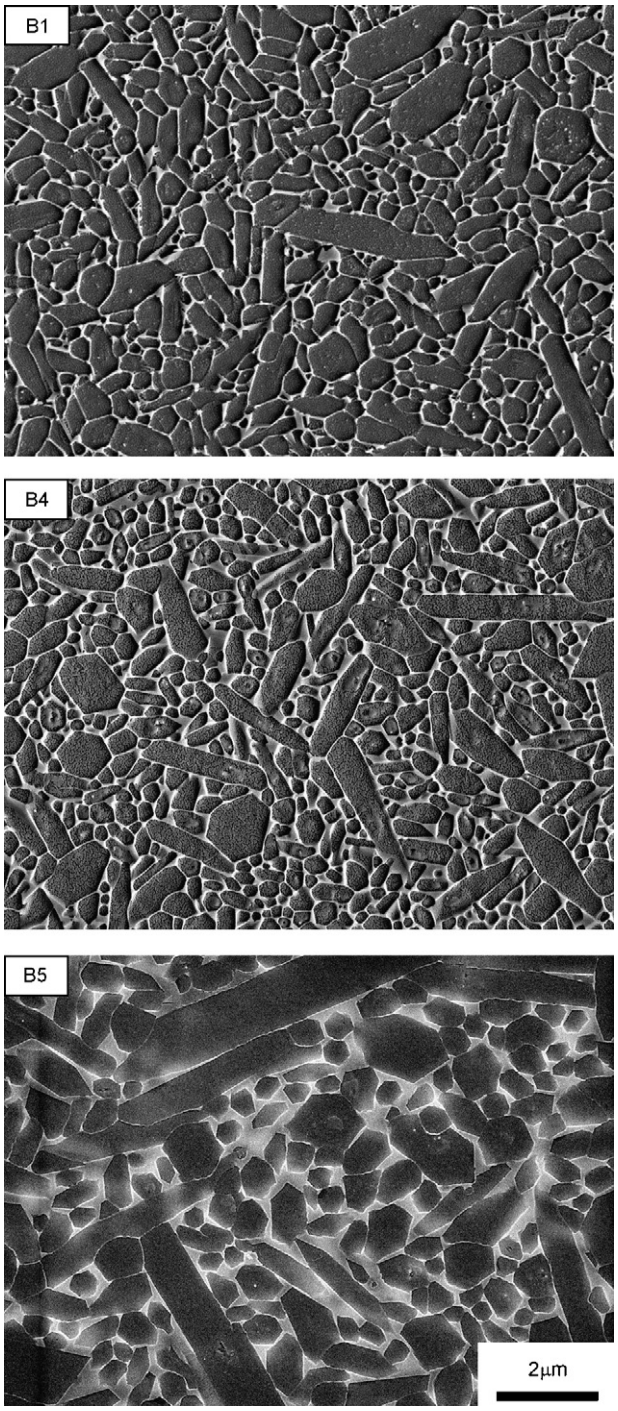

Fig. 2. SEM micrographs of Si_3N_4 hot-pressed at 1950 °C for 2 h with addition of various amounts of sintering aids. The amounts of Al_2O_3 and Y_2O_3 as sintering additives were 1.0 and 1.0 wt% (B1); 3.34 and 3.34 wt% (B4); 10.0 and 10.0 wt% (B5); respectively.

of the coarse grains selected from the micrographs of 1k magnification images were mostly ∼10 as listed in Table 1, while other normal grains showed the aspect ratio of 4–6, indicating that only small number of grains experienced unidirectional and noticeable grain growth.

XRD analysis identified only β-phase for all the samples with the exception of the A1 sample in which the slight amount

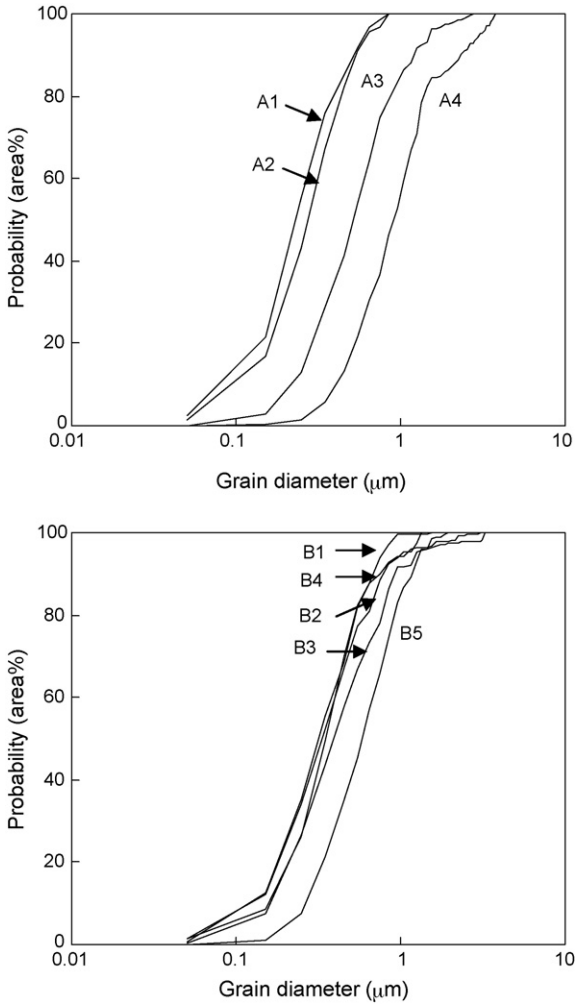

Fig. 3. Distributions of grain diameter for Si_3N_4 ceramics hot-pressed with Al_2O_3 and Y_2O_3 as sintering aids. The letter by every curve represents the sample designation listed in Table 1.

of residual α phase was detected. The absence of secondary crystalline phase in these samples indicated that the sintering additives formed intergranular glassy phases.

3.2. Hardness, fracture toughness and wear behavior

Table 2 summarizes the basic mechanical properties such as Young's modulus, hardness and fracture toughness as well as specific wear rate for the silicon nitride samples with different microstructures. The change in Young's modulus among the samples in the A group was negligible. By contrast, the Vickers hardness, H of the samples in the A group showed decreasing tendencies with an increase in the sintering temperature and soaking time, which may be partially attributable to the size effect as reported in other hot-pressed silicon nitride ceramics.[10,29,30] In the case of B samples, both Young's modulus and H decreased gradually with an increase in the amount of additives, which can be explained by the increase in the volume fraction of intergranular phase that is softer than pure Si_3N_4 phase. Both fracture toughness, K_{Ic} measured by the SEPB method and fracture resistance, K_R calculated from the IF tech-

Table 2
Mechanical properties and average of the specific wear rate for silicon nitride samples with different microstructures

Material designation	Young's modulus (GPa)	Vickers hardness (H, GPa)[a]	Fracture toughness (K_{Ic}, MPa m$^{1/2}$)	Fracture resistance (K_R, MPa m$^{1/2}$)[b]	Specific wear rate ($\times 10^{-4}$ mm^3 N^{-1} m^{-1})
A1	299	15.2 ± 0.1	5.2 ± 0.1	4.9 ± 0.1	4.40
A2	299	14.8 ± 0.1	5.7 ± 0.04	5.4 ± 0.1	1.90
A3	300	14.1 ± 0.1	7.0 ± 0.1	5.9 ± 0.1	0.28
A4	306	13.6 ± 0.1	8.3 ± 0.2	6.6 ± 0.1	0.45
B1	315	15.9 ± 0.3	4.5 ± 0.1	4.2 ± 0.1	4.00
B2	312	15.7 ± 0.2	4.9 ± 0.2	4.7 ± 0.1	2.10
B3	309	14.8 ± 0.2	6.5 ± 0.1	5.7 ± 0.1	0.06
B4	307	14.8 ± 0.1	6.5 ± 0.2	5.9 ± 0.1	0.06
B5	280	13.6 ± 0.1	7.0 ± 0.3	6.0 ± 0.1	0.75

[a] Vickers hardness was measured at an indentation load of 294 N.
[b] Fracture resistance was obtained by the indentation fracture (IF) method at a load of 294 N. Uncertainties are one standard deviation.

nique increased with the sintering temperature and holding time for the samples in the A group. The samples in B group showed an increase in both K_{Ic} and K_R with the content of additives. It is rational to expect that the crack bridging mechanism is responsible for the enhanced K_{Ic} and K_R in the samples sintered at higher temperatures and with large amount of additives since the volume fraction of the coarse and elongated grains increased in these samples as mentioned above (Figs. 1–3).[31,32] It should be noted that the discrepancy between K_{Ic} and K_R became evident when the large needle-like grains dominated the microstructure of those samples sintered at high temperature and/or with abundant additives (A3, A4 and B5 samples). This phenomenon was reported previously by the authors and was discussed in conjunction with the difference in the effective crack-bridging length,[26,27] that is, K_{Ic} represents the fracture resistance at the relatively long bridging length in the R-curve plots, whereas IF method measures the K_R value at the shorter bridging length.

The specific wear rate, W_s, in this study showed a significant variation of about two orders of magnitude (from 6×10^{-6} to $\sim 4 \times 10^{-4}$ mm^3 N^{-1} m^{-1}) (Table 2). Fig. 4 shows the relationship between the specific wear rate, W_s and median grain diameter of the samples. The specific wear rates are also plotted against the Vickers hardness and the fracture resistance in Figs. 5 and 6, respectively. It is obvious that there were no correlations between them.

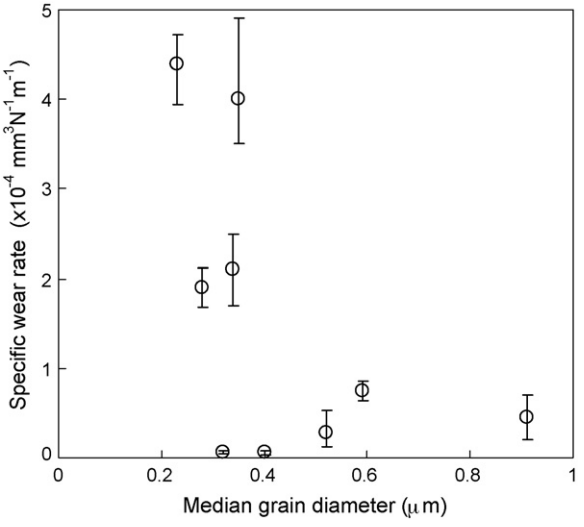

Fig. 4. Specific wear rate versus median grain diameter for Si_3N_4 ceramics hot-pressed with Al_2O_3 and Y_2O_3 as sintering aids. Vertical error bars indicate the ranges of measured values.

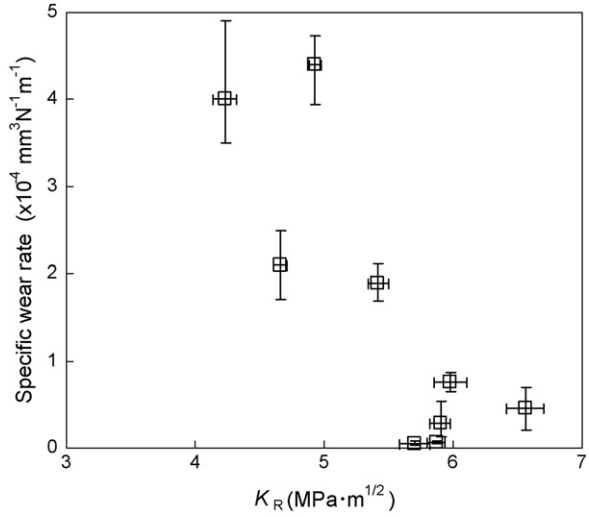

Fig. 5. Specific wear rate versus fracture resistance, K_R for Si_3N_4 ceramics hot-pressed with Al_2O_3 and Y_2O_3 as sintering aids. K_R was obtained by the IF method at an indentation load of 294 N. Horizontal error bars are ±1 standard deviation. Vertical error bars indicate the ranges of measured values.

4. Discussion

Evans and Marshall developed a lateral-crack chipping model to quantitatively analyze the mechanism of material removal in abrasive machining of brittle ceramics,[19] in which material removal rate, ΔV caused by a passage of each grinding particle is related to the peak normal penetration forces, P_n, Vickers hardness, H and fracture toughness, K_{Ic} as follows:

$$\Delta V \propto \frac{P_n^{9/8}}{(K_{Ic}^{1/2} H^{5/8})} \quad (2)$$

In this study, there were no grinding particles which are used in their model. However, our previous studies observed the typical morphology of abrasive wear with particulate debris on the

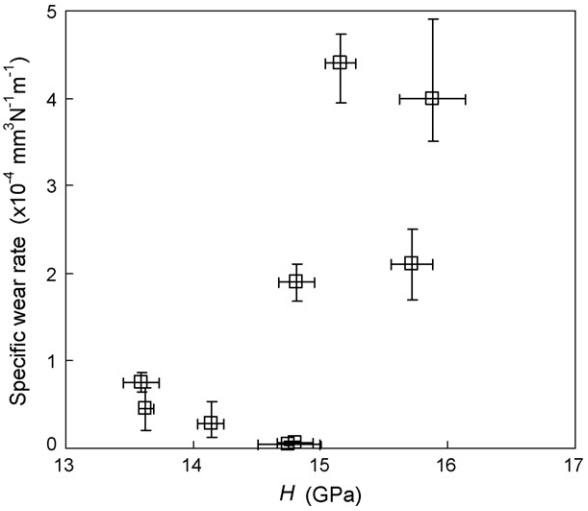

Fig. 6. Specific wear rate versus Vickers hardness, H for Si_3N_4 ceramics hot-pressed with Al_2O_3 and Y_2O_3 as sintering aids. H was obtained at an indentation load of 294 N. Horizontal error bars are ±1 standard deviation. Vertical error bars indicate the ranges of measured values.

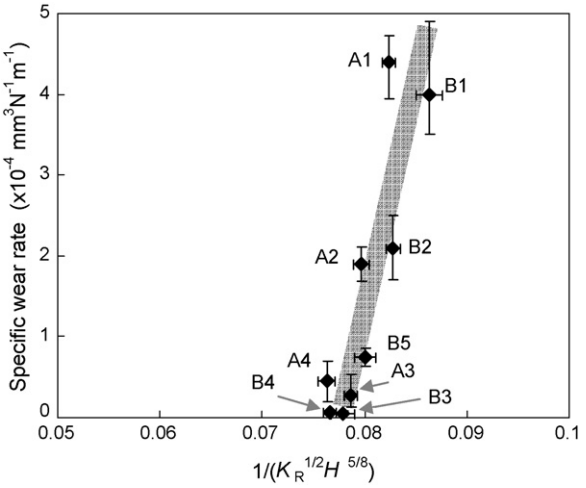

Fig. 7. The relationships between the specific wear rate and $1/(K_R^{1/2}H^{5/8})$ for Si_3N_4 ceramics hot-pressed with Al_2O_3 and Y_2O_3 as sintering aids. Fracture resistance, K_R was obtained by the IF method at an indentation load of 294 N (K_R is given in MPa m$^{1/2}$ and H is given in GPa). Horizontal error bars are ±1 standard deviation. Vertical error bars indicate the ranges of measured values. The letter by each data point represents the sample designation.

worn surfaces for all of the samples in this study.[17,18] It is likely that the a large piece of Si_3N_4 debris was formed by a grain dropping due to the abrasive wear and acted as a sharp indenter since the rough surfaces of the worn areas for all the samples were indicative of abrasive wear. If this is the case, the model can be reasonably applied to this study. The peak normal force for each grinding particle, P_n, can be estimated by dividing the normal load, F_n, by the number of such a large piece of Si_3N_4 debris, N. The total wear loss, V is derived by the products of ΔV and N. The specific wear rate, W_s, is given by $V/(F_nL)$ where normal load, F_n and sliding distance, L are constants in this study. Then, the next equation is obtained.

$$W_s = \frac{(\Delta VN)}{(F_nL)} \propto \frac{(F_n/N)^{9/8}}{K_{Ic}^{1/2}H^{5/8}} \times \frac{N}{F_nL} = \frac{(F_n/N)^{1/8}}{K_{Ic}^{1/2}H^{5/8}} \times \frac{1}{L} \quad (3)$$

In this study, it is assumed that the number of large Si_3N_4 debris, N is almost the same among the samples. Thus, Eq. (3) is simplified as follows:

$$W_s \propto \frac{\alpha}{K_{Ic}^{1/2}H^{5/8}} \quad (4)$$

where α is constant ($\alpha = N^{-1/8}F_n^{1/8}L^{-1}$).

In Fig. 7, the specific wear rates, W_s, are plotted against $1/(K_R^{1/2}H^{5/8})$ using the fracture resistance measured by the IF method. A clear correlation between the W_s and $1/(K_R^{1/2}H^{5/8})$ was obtained. By contrast, the good correlation was lost when the fracture toughness, K_{Ic}, obtained by the SEPB method was used instead of K_R (Fig. 8). When Fig. 8 is compared with Fig. 7, the shifts of the data points in the X-axis for the A3, A4 and B5 samples were much distinct than those of other samples, which made the correlation worse. The large shifts in the X-axis for the A3, A4 and B5 samples were originated from the discrepancies between the values of K_{Ic} and K_R, which can be explained by the steep rising R-curve behavior for these samples. It is clear that the K_{Ic} obtained at long crack length was inappropriate to analyze the wear behavior with this model. By contrast, K_R obtained by the IF method was preferable to correlate the wear properties with H and K_R. The crack length of indentation at 294 N ranged between 250 and 310 μm, which was significantly smaller than that of SEPB, ~2 mm. Doğan and Hawk reported that the subsurface cracking parallel to the surface in the silicon nitride after the abrasive test was ~100 μm.[12] Although the crack size measured by the IF method was still larger than the length of the subsurface cracking reported by Doğan and Hawk, it is reason-

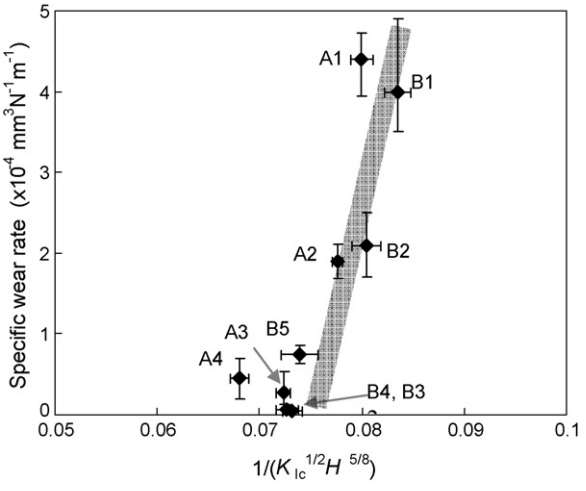

Fig. 8. The relationships between the specific wear rate and $1/(K_{Ic}^{1/2}H^{5/8})$ for Si_3N_4 ceramics hot-pressed with Al_2O_3 and Y_2O_3 as sintering aids. Fracture toughness, K_{Ic} was obtained by the SEPB method (K_{Ic} is given in MPa m$^{1/2}$ and H is given in GPa). Horizontal error bars are ±1 standard deviation. Vertical error bars indicate the ranges of measured values. The letter by each data point represents the sample designation.

able to deduced that the K_R from IF is superior in analyzing the localized damage to the K_{Ic} from SEPB.

It seems that the material removal process in this wear study can be explained by the lateral fracture mechanism. However, when you look closer at Fig. 7, it appears that most of the data points of samples in the A group located left side of the thick gray line, whereas those for the B samples resided in the opposite side. And furthermore, the line in Fig. 7 did not intercept the origin. Xu et al. successfully applied the lateral-crack chipping model to predict the abrasive wear behavior by using the short-crack toughness.[33] They found a correlation between the normal grinding force and the inverse function of fracture resistance and hardness. However, the extrapolations of the best-fit lines did not go through the origin. Other researchers have shown that the Evans–Marshal model failed to adequately describe the tribological behavior of some silicon nitrides with different microstructures.[10–12] For example, it was reported that the volume wear loss of a silicon nitride sample whose grain boundary phase was fully crystallized was much larger than those of silicon nitrides with intergranular glassy phase.[12] Doğan and Hawk attributed the difference to the severe residual stress in the former sample caused by the mismatch of thermal expansion between the matrix and the second crystalline phase.[12] Theses suggests that a term which deals the residual stress between grains may be necessary in Eq. (2) and/or that the exponents for hardness and fracture resistance for the microfracture process may be different from those for the lateral-crack chipping model in Eq. (2). Therefore, a new comprehensive model for wear mechanism in the unlubricated slicing test is needed to clarify the effect of microstructure on the wear behavior.

5. Summary

The effect of fracture resistance on the tribological behavior of silicon nitride ceramics was studied using nine samples with progressively coarsened microstructures. Both hardness and fracture resistance did not show any direct relationship to the specific wear rate measured in the ball-on-disk test, individually. An indentation fracture model for material removal process was used to correlate the wear behavior with the inverse function of fracture resistance and hardness of the materials. An agreement was obtained between the experimental results and the indentation model when the indentation fracture resistance was employed instead of the fracture toughness obtained by the SEPB method. This suggested that both indentation fracture resistance and hardness is useful for ranking the wear resistance of Si_3N_4 with various microstructures.

Acknowledgment

This work has been supported by METI, Japan, as part of the international standardization project of test methods for rolling contact fatigue and fracture resistance of ceramics for ball bearings.

References

1. Blau, P. J., Effects of surface preparation on the friction and wear behavior of silicon nitride/silicon carbide sliding pairs. *J. Mater. Sci.*, 1992, **27**, 4732–4740.
2. Gee, M. G. and Butterfield, D., The combined effect of speed and humidity on the wear and friction of silicon nitride. *Wear*, 1993, **162–164**, 234–245.
3. Dong, X. and Jahanmir, S., Wear transition diagram for silicon nitride. *Wear*, 1993, **165**, 169–180.
4. Kitaoka, S., Tsuji, T., Katoh, T., Yamaguchi, Y. and Sato, K., Effect of sintering aids on tribological characteristics of Si_3N_4 ceramic at 120 °C in water. *Wear*, 1994, **179**, 63–67.
5. Kim, S. S., Kim, S.-W. and Hsu, S. M., A new parameter for assessment of ceramic wear. *Wear*, 1994, **179**, 69–73.
6. Skopp, A., Woydt, M. and Habig, K.-H., Tribological behavior of silicon nitride materials under unlubricated sliding between 22 °C and 1000 °C. *Wear*, 1995, **181–183**, 571–580.
7. Ravikiran, A. and Bai, B. N. P., Influence of speed on the tribological reaction products and the associated transitions for the dry sliding of silicon nitride against steel. *J. Am. Ceram. Soc.*, 1995, **78**, 3025–3032.
8. Wang, Y. and Hsu, S. M., Wear and wear transition mechanisms of ceramics. *Wear*, 1996, **195**, 112–122.
9. Zanoria, E. S. and Blau, P. J., Effect of incidence angle on the impact-wear behavior of silicon nitride. *J. Am. Ceram. Soc.*, 1998, **81**, 901–909.
10. Zutshi, A., Haber, R. A., Niesz, D. E., Adams, J. W., Wachtman, J. B., Ferber, M. K. and Hsu, S. M., Processing, microstructure, and wear behavior of silicon nitride hot-pressed with alumina and yttria. *J. Am. Ceram. Soc.*, 1994, **77**, 883–890.
11. Gomes, J. R., Oliveira, F. J., Silva, R. F., Osendi, M. I. and Miranzo, P., Effect of α-/β Si_3N_4-phase ratio and microstructure on the tribological behavior up to 700 °C. *Wear*, 2000, **239**, 59–68.
12. Doğan, C. P. and Hawk, J. A., Microstructure and abrasive wear in silicon nitride ceramics. *Wear*, 2001, **250**, 256–263.
13. Carrasquero, E., Bellosi, A. and Staia, M. H., Characterization and wear behavior of modified silicon nitride. *Int. J. Refractory Metal Hard Mater.*, 2005, **23**, 391–397.
14. Wang, D. and Mao, Z., Studies on abrasive wear of monolithic silicon nitride and a silicon carbide whisker-reinforced silicon nitride composite. *J. Am. Ceram. Soc.*, 1995, **78**, 2705–2708.
15. Doğan, C. P. and Hawk, J. A., Influence of whisker reinforcement on the abrasive wear behavior of silicon nitride- and alumina-based composites. *Wear*, 1997, **203/204**, 267–277.
16. Gomes, J. R., Osendi, M. I., Miranzo, P., Oliveira, F. J. and Silva, R. F., Tribological characteristics of self-mated couples of Si_3N_4-SiC composites in the range 22–700 °C. *Wear*, 1999, **233–235**, 222–228.
17. Hyuga, H., Hirao, K., Yamauchi, Y. and kanzaki, S., The influence of microstructure and mechanical properties on the friction and wear behavior of Si3N4 ceramics. In *Proceedings of the second world tribology congress, published by CD-ROM*, 2001.
18. Hyuga, H., Hirao, K., Yamauchi, Y. and kanzaki, S., Influence of microstructure and grain boundary phase on tribological behavior of Si_3N_4 ceramics. *Ceram. Eng. Sci. Proc.*, 2001, **22**, 197–202.
19. Evans, A. G. and Marshall, D. B., Wear mechanisms in ceramics. In *Fundamentals of Friction and Wear of Materials*, ed. D. A. Rigney. American Society for Metals, Metals Park, OH, 1981, pp. 439–452.
20. Mitomo, M., Tsutsumi, M. and Tanaka, H., Grain growth during gas-pressure sintering of β-silicon nitride. *J. Am. Ceram. Soc.*, 1990, **73**, 2441–2445.
21. *Testing Methods for Elastic Modulus of Fine Ceramics*, Japanese Industrial Standard, JIS R 1602, 1995.
22. *Testing Methods for Fracture Toughness of Fine Ceramics*, Japanese Industrial Standard, JIS R 1607, 1995.
23. Miyoshi, T., Sagawa, N. and Sasa, T., Study of evaluation for fracture toughness of structural ceramics. *J. Jpn. Soc. Mech. Eng. A*, 1985, **51**, 2489–2497.
24. Quinn, G. D., Fracture toughness of ceramics by the Vickers indentation crack length method: a critical review. *Ceram. Eng. Sci. Proc.*, 2006, 27.

25. Quinn, G. D. and Bradt, R. C., On the Vickers indentation fracture toughness test. *J. Am. Ceram. Soc.*, 2007, **90**, 673–680.
26. Miyazaki, H., Hyuga, H., Hirao, K. and Ohji, T., Comparison of fracture resistance measured by IF method and fracture toughness determined by SEPB technique using silicon nitrides with different microstructures. *J. Eur. Soc. Ceram.*, 2007, **27**, 2347–2354.
27. Miyazaki, H., Hyuga, H., Hirao, K. and Ohji, T., Relationship between fracture toughness determined by surface crack in flexure and fracture resistance measured by indentation fracture for silicon nitride ceramics with various microstructures. *Ceram. Int.*, in press.
28. *Testing Method for Wear Resistance of High Performance Ceramics by Ball on Disk Method*, Japanese Industrial Standard, JIS R 1613, 1993.
29. Babini, G. N., Bellosi, A. and Galassi, C., Characterization of hot-pressed silicon nitride-based materials by microhardness measurements. *J. Mater. Sci.*, 1987, **22**, 1687–1693.
30. Mukhopadhyay, A. K., Datta, S. K. and Chakraborty, D., Hardness of silicon nitride and sialon. *Ceram. Int.*, 1991, **17**, 121–127.
31. Becher, P. F., Microstructural design of toughened ceramics. *J. Am. Ceram. Soc.*, 1991, **74**, 255–269.
32. Steinbrech, R. W., Toughening mechanisms for ceramic materials. *J. Eur. Ceram. Soc.*, 1992, **10**, 131–142.
33. Xu, H. H. K., Jahanmir, S., Ives, L. K., Job, L. S. and Ritchie, K. L., Short-crack toughness and abrasive machining of silicon nitride. *J. Am. Ceram. Soc.*, 1996, **79**, 3055–3064.